Development of a hydrogen producing Ceria based demonstration plant coupled to a 200 kW$_{th}$ solar simulator

St. Breuer[1], C. Spenke[1], M. Wullenkord[1], J.-P. Säck[1], M. Roeb[1], Chr. Sattler[1]

[1]German Aerospace Center (DLR), Institute of Solar Research, Linder Hoehe 51147 Köln, Germany
email: stefan.breuer@dlr.de

Abstract

DLR is building the world's biggest solar simulator in Jülich, Germany, with a thermal power output of around 200 kW. A hydrogen production unit was chosen to be the very first experiment to be set up. Ceria is a promising redox material for two-step thermochemical water-splitting. The well-known, directly irradiated cavity design, successfully used in other CSP projects DLR contributed to, seems appropriate for a high-temperature ceria based reactor. The required temperature for water-splitting is around 1100 °C, while the regeneration step takes place at 1400 °C. To adapt the cavity design to the new conditions, a thermodynamic analysis of this reactor as well as the necessary reactor design changes were carried out, i.e. the window design and its high temperature sealing. The cavity, designed as a dome composed of ceria-foams, is developed for 1400 °C and will be assembled with high temperature stable ceramic compound stripes. Additionally, a parametric study is carried out, together with the foam manufacturer, to detect the most suitable ceria form for foam shaping.

Keywords: *solar, chemical engineering, hydrogen, ceria-oxide, reactor development*

1 Introduction

The extensive use of regenerative energies, especially solar thermal power, leads to challenges if it is to become a reliable, competitive electricity producer. The concentrated solar power technology's big advantage, compared to other renewable energy sources, is that its intermittency can be compensated by storing the heat. This storing could be provided by the generation of hydrogen.

A possibility of producing hydrogen is a solar-powered thermo-chemical cycle. One two-step cycle, based on a metal oxide redox pair system, can split water molecules by absorbing oxygen atoms and reversibly incorporating them into its lattice has been developed [1].

The cycle's first step is the oxidation of the metal oxide layer with a high temperature steam flow, between 800 °C and 1100 °C: the oxide captures the oxygen from the water and thus the hydrogen is released. The oxygen capture is very important because elsewise the separated molecules would spontaneously recombine to water.

$$MO_{red} + H_2O \rightarrow MO_{ox} + H_2 \qquad (1)$$

The second step, the regeneration of the oxidised metal oxide and takes place at temperature between 1100 °C and 1400 °C in an atmosphere with a low O$_2$ partial pressure (i.e. N$_2$ or vacuum): at these conditions the metal oxide releases the captured oxygen and can be oxidised again, closing the cycle [2].

$$MO_{ox} \rightarrow MO_{red} + \frac{1}{2}O_2 \qquad (2)$$
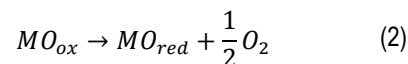
The heat power for this reaction will be obtained by concentrating solar radiation onto a receiver. This receiver could be placed on a solar tower power plant.
The redox pair chosen for this reactor for this cycle is ceria-oxide, which sounds very promising in lab-scale. Ceria is a non-stoichiometric redox material and is able to split H$_2$O and CO$_2$.[3]
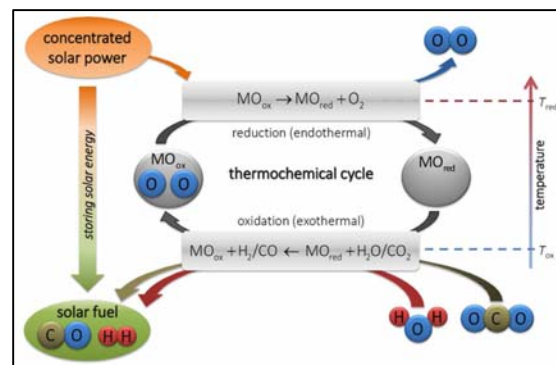The general schematic of the two-step thermochemical cycle is shown in the following figure.

Fig. 1: General schematic of the two-step thermochemical cycle for H$_2$O/CO$_2$ splitting

Within this paper, the general ability of Ceria will be explained as well as the adapted reactor's geometry. Furthermore, a simplified thermodynamic model for calculating the heat balance will be introduced. These results are the preparation for the upcoming experimental campaign, which follows in the year 2016.

2 Redox material

Despite the successful experimental campaigns within the HYDROSOL 2 project, that approved the operability of that process, identification of a suitable material is still a major technical barrier [4, 5]. Recently ceria emerged as a promising material [6, 7]. Using ceria oxide, which is a non-stoichiometric redox material, seems to have several benefits. First of all, it is able to split water and CO_2 and additionally, ceria oxide has beneficial kinetics in comparison to other mixed oxides for redox reactions. The reaction is slightly different, compared to the above mentioned. Both of the H20 splitting cycle equations, for high temperature

$$CeO_2 \rightarrow CeO_{2-\delta} + \frac{\delta}{2} O_2 \qquad (3)$$
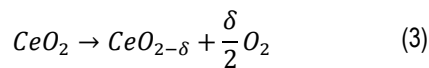
and low-temperature are shown in the following:

$$CeO_{2-\delta} + \delta H_2O \rightarrow CeO_2 + \delta H_2 \qquad (4a)$$

$$CeO_{2-\delta} + \delta CO_2 \rightarrow CeO_2 + \delta CO \qquad (5b)$$
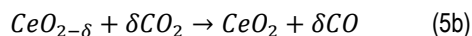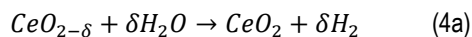
The reduction of CeO2 occurs at high temperatures and/or at low oxygen partial pressures by forming oxygen vacancies as a logical consequence of the oxygen release. The resulting non-stoichiometric ceria is characterised by the sub-oxide parameter δ applying T/p_{O2} conditions [8]. Subsequently, re-oxidation of $CeO_{2-\delta}$ in the presence of H_2O causes its splitting [3].
In comparison to the direct method of H_2 generation from water, which happens at 4000 °C, the thermo-chemical cycles are more efficient in terms of temperature [9]. Especially the two step thermo-chemical cycles have drawn great attention in the last decades and they are more and more focused in research application [10].
Even though, doped ceria seems to provide better results in generating hydrogen and carbon-monoxide, it was chosen to not use those doped materials [10]. This is mainly because of the unknown stability of the doped material as it has to be used in an up-scaled process for 200 kW_{th} within this project. For the biggest ever built ceria based water-splitting test-reactor it is considered less risky to rely on a material, which is better known in technical terms and for which more knowledge is available in terms of bringing it into a foam shape. Within this project a pre-study for using the doped ceria was conducted, with the outcome that it seems possible to use such materials.
Another small scale study showed the very good thermal stability of pure ceria, in both mechanical stress and shrinkage. The foam was thermos-gravimetrically analysed at 23 cycles within a temperature range of

around 1000 °C and 1400 °C. A very small weight loss of around 15 mg was detected, at a total mass of 6189 mg at the beginning and 6173 mg after the analysis. Fig. 2 shows the ceria foams after analysis (left hand side) and before tests (right hand side).
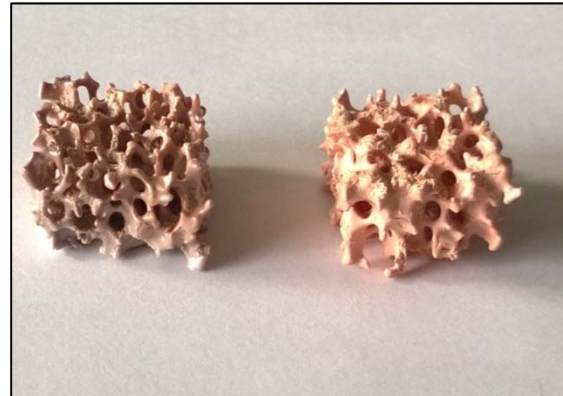

Fig. 2: Ceria foams after and before thermal analysis

3 Reactor Geometry

In this project a well-known reactor concept, used in former projects, has been refined. This was necessary because of the new challenges the reactor has to meet. The particular reactor requirements in this project are:

- Reach temperatures up to 1.400°C at the ceramic redox absorber
- Operate with an incidence angle of radiation from 0° to 60°, received from the solar simulator
- Use a larger quantity of active redox ceramic material, in this case ceria, as a promising redox material

Fig. 3 shows a scheme of the new reactor, which is designed for chemical water-splitting. The reactor is driven with a maximum pressure of 1.5 bar_a. The reactor consists of a volumetric absorber, a quartz window and a system of three vessels. The external vessel, with an external diameter of 1100 mm, separates the inside of the reactor from the ambient. Its inner surface is insulated with a special high temperature insulation material, to keep the reactor's thermal losses low. The middle vessel shields the insulation layer from the inlet gas stream. The inner vessel separates the inlet and outlet flow. The length of the complete reactor included the gas connection at the back side is about 1600 mm. Because of the high incidence angle of irradiation, up to 60°, a secondary concentrator could not be used. A secondary concentrator has to main tasks: First to shield the window flange from irradiation and second to increase the solar flux density into the reactor aperture. Instead of the secondary concentrator a ring of water cooled secondary extensions are mounted to protect the window gasket and the absorber foundation against direct irradiation.
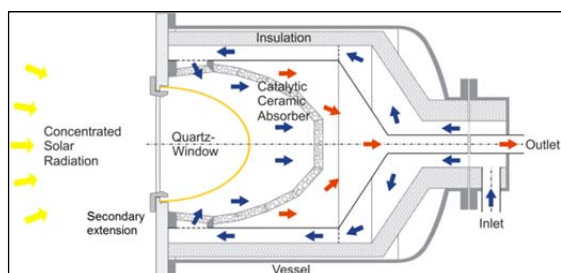
2

Fig. 3: Scheme of the reactor

The reactor aperture with a diameter of 600 mm is covered by a dome-shaped quartz window. At the window surface reflected rays have the chance of hitting the window a second time and thus transmit through the window. The radiation, transmitted through the quartz window, is absorbed on the cavity shaped volumetric absorber. By reason of this absorber shape, the losses due to the irradiation from the absorber to the ambient could be decreased. For the required ceria quantity of about 90 dm³ the material thickness of the absorber foams was increased to 60 mm and thus geometry was optimized. This leads to an absorber dome, which is now assembled of 109 ceria-foam segments with a density of around 1.4 g/cm³. A ring of 18 segments close the window flange forms the inlet absorber. Separated from the inlet absorber by a gas-tight dividing layer, made of alumina, five rings of 18 segments and a center disk are used to build the outlet absorber. The absorber is made of pure Ceria, so no carrier structure for the ceria is needed. All foam parts are positioned by a system of high temperature stable ceramic compound stripes, which guarantee a sufficient temperature resistance up to 1400°C. Furthermore, these stripes keep the absorber in shape. The inner diameter of the absorber dome is 662 mm and the length of the inside surface of the cavity has a value of 661 mm.

The stream of process gas is launched in the reactor between the middle and inner vessel. Hereby the hot section in the inner vessel gets an additional thermal isolation from the environment and additionally the inlet gas will be preheated by the outlet flow. As a result of this, the thermal losses are reduced and the operating temperature increased.

Afterwards, the flow passes through the inlet absorber ring into the cavity, where it is heated by the radiation hitting the absorber surface. While flowing through outlet absorber and getting in contact with the ceria foams, the stream of gas reaches the highest temperature and the chemical reaction takes place. This heat balance will be described further in the thermodynamic analysis.

During the stage of water splitting and hydrogen production the reaction needs a temperature level of between 800 °C to 1100 °C. Whereas, the regeneration step, while freeing oxygen, requires the highest temperature from 1100 °C up to 1400 °C for the best efficiency. The temperature values will be tested in a parametric study during the experimental campaign.

After this, the stream flows through the inner vessel into the outlet pipe, with a following heat recovery and gas analysis.

A sectional view of the reactor in an advanced stage of the project is shown in Fig. 4.
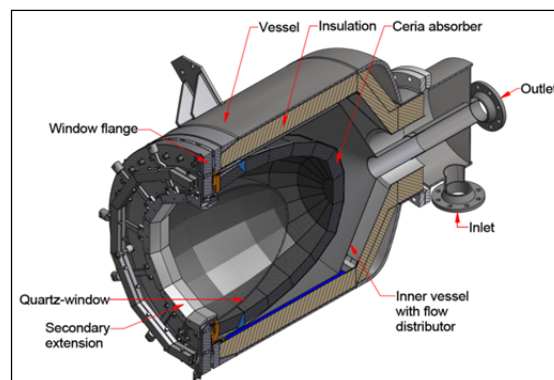

Fig. 4 Sectional view of the reactor

4   Thermodynamic model

Temperatures of the redox material as high as 1400 °C should be reached in order to allow efficient regeneration. A simplified, stationary, thermal model of a possible configuration of the water splitting reactor was elaborated. Furthermore, it was analysed with respect to relevant heat flows, aiming at the estimation of probable temperatures of the absorber structure and the reactor window in operation. As can be seen in Fig. 3 the reactor configuration chosen for an initial assessment features a hemispheric absorber dome (A) covered by a planar quartz window (W, 650 mm diameter, 15 mm thickness) at the front. A real thermal isolation material (I) between the outer surface of the absorber dome and the ambience (Amb) reduces thermal losses in radial direction. Any temperature gradients in the window, in the absorber, and the ambience are neglected. The gap between the front face of the absorber/isolation assembly and the peripheral face of the window is filled with an ideal thermal isolation material (I_{ideal}). This leads to a disregard of any heat transport at respective surfaces. The temperature of the inner surface of the real thermal isolation material is set to absorber temperature, whereas the temperature of the outer surface is set to ambient temperature. During the regeneration phase a nitrogen flow (N_2), which is pre-heated in a heat recovery module (HR), is introduced to the reactor through a virtual gap between window and absorber. The pre-heated nitrogen interacts with the inner surface of the window before approaching the absorber, where it receives the final heat input to reach absorber temperature. The hot nitrogen leaves the absorber and enters the heat recovery module. There, part of the thermal energy of the hot gas flow is used to pre-heat the cold nitrogen flow entering the system as described above. The heat needed to drive the chemical regeneration reactions in the absorber is neglected. In

3

this model the temperature of the absorber and the temperature of the window are varied in order to meet the requirement of balanced energy flows in stationary mode of both, the absorber and the window. The heat flows associated to radiation, convection, and conduction are analysed in the following.
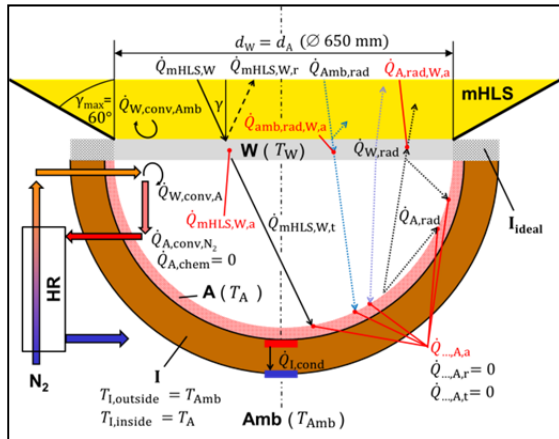

Fig. 5: Simplified model of the reactor with the absorber material (A), the quartz window (W), the isolation material (I), the ideal isolation material (I_{ideal}), the ambience (Amb), the heat recovery module (HR), and various heat flows. (conv: convective, rad: radiative, cond: conductive, r: reflected, a: absorbed, t: transmitted)

Radiation

The reactor window receives a radiative energy input from the high flux solar simulator (mHLS). Due to spillage (20% assumed in the reference case) the heat flux striking the window is lower than the power emitted by the mHLS. In this preliminary assessment it is presumed that geometry and positioning lead to a maximum angle of incidence of 60°. The mHLS is implemented as a spherical calotte with rim angles of 60°, acting as a uniform 200 kW_{th} source of black-body radiation at 5500 °C. The centre of the considered calotte corresponds to the centre of the outer circular surface of the window. The spherical calotte was divided into subdomains characterised by an angle interval of 5°. For each interval an effective angle of incidence was defined, which leads to two subdomain fragments with equal surfaces. Depending on the angle of incidence and the considered wavelength different fractions of incoming light are transmitted (to the absorber), reflected or absorbed from the reactor window. According to 12 intervals of 5° dividing the calotte, 12 effective angles of incidence were calculated along with the ratios of the represented subdomain surface to the total surface of the spherical calotte. Based on findings of the project Effective optical properties, i.e. reflectance, transmittance, and absorptance of the applied quartz window (at window temperature) are estimated in the range from 0.25 µm to 80 µm with a resolution of 0.01 µm. The radiation emitted by the mHLS is calculated for the specified wavelength regime employing Planck's law for the spectral radiant exitance of a black-

body at 5500 °C. Using the effective reflectance, transmittance, and absorptance of quartz at window temperature the radiative flux from the mHLS striking the window can be split into a reflected, transmitted, and absorbed fraction. The transmitted fraction approaches the volumetric absorber modelled with perfect absorption and emissivity. Therefore, the absorber neither reflects nor transmits any incoming radiation. The black-body radiation emitted by the absorber is calculated using Planck's law for the spectral radiant exitance of a black-body at absorber temperature. The following view factors of the absorber/window assembly can be calculated: φ_{AA} = 0.5, φ_{AW} = 0.5, φ_{WA} = 1, and φ_{WW} = 0. As a result 50% of the power emitted by the absorber is directly absorbed by the absorber again. The remaining fraction hits the window and is partly transmitted, absorbed, and reflected, respectively. The reflected fraction reaches the absorber where it is completely absorbed. In this context the effective reflectance, transmittance, and absorptance of the quartz window is calculated as described above. Angular characteristics, however, are approximated by a spherical (absorber) calotte with 90° rim angles instead of a spherical (mHLS) calotte with 60° rim angles. The same angular characteristics are used to address the radiative input to the window/absorber-assembly from the ambience at ambient temperature. Finally the window emits radiation to the absorber and to the ambience. In contrast to the mHLS and the absorber the assumption of black-body behaviour is not applicable for the window. The spectral radiant excitance of a black-body at window temperature is modified by the effective emissivity which was approximated by the effective absorptance of the window.

Convection

During the regeneration phase, nitrogen flows through the reactor. Part of the energy needed to heat the nitrogen flow up to absorber temperature is provided by the heat recovery module. Concerning the reference case, 30% of the energy is inserted by heat recovery. The convective heat transport at the inner surface of the window is considered employing Nusselt correlations for combined forced and free convection. The third heat flux required to reach absorber temperature is extracted from the absorber. The outer surface of the window is cooled by the contact to the ambient air assessed by Nusselt correlations for free convection. The employed Nusselt correlations were used in accordance with [11].

Conduction

It was assumed that the real isolation material covering the outer surface of the absorber is characterised by a thermal conductivity of 1 W/(m K). The conductive heat flux through the isolation is calculated for the temperature gradient mentioned above approximating the relevant heat transfer surface by the average of the inner and outer surface of the isolation dome. Since the temperature of the outer surface of the isolation material

4

is set to ambient temperature an ideal convective heat transport to the ambience is presumed.

5   Result and discussion

The reference case of the reactor simulation is specified by 200 kW_{th} initial power of the mHLS, 20% spillage, 30% heat recovery fraction, 100 kg/h nitrogen flow, 100 mm isolation thickness, 40 mm absorber thickness, and 25 °C ambient temperature. Under these conditions an absorber temperature of 1418 °C and a window temperature of 1054 °C can be calculated. Detailed means of power yield and losses of the window are presented in Fig. 6. Absorbed radiation emitted by the absorber is the dominant source of heat representing 85% of the input. Compared to radiative heat transfer convective effects are of minor importance.
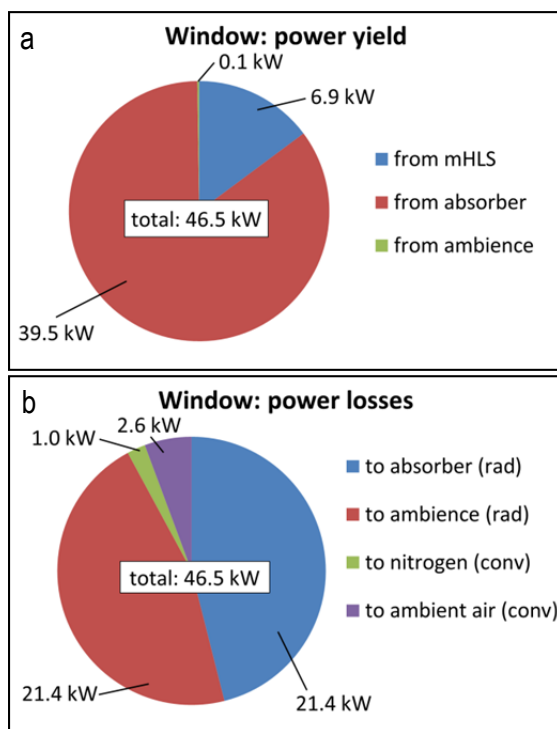

Fig. 6: Simulation results concerning the power yield (a) and losses (b) of the window regarding the reference case

Detailed means of power yield and losses of the absorber are shown in Fig. 7. The major power input originates from the mHLS. Power losses are mainly attributed to radiative heat transfer to the window and the ambience. However, convection and conduction contribute significantly to the total loss of 198.9 kW.
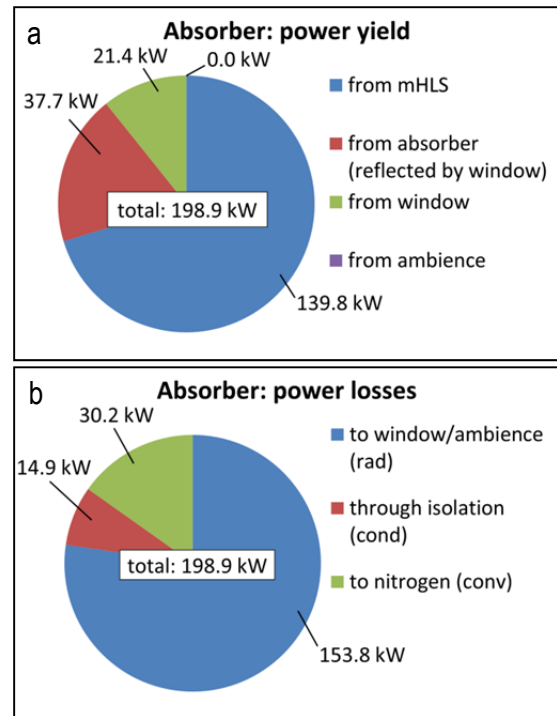

Fig. 7: Simulation results concerning the power yield (a) and losses (b) of the absorber regarding the reference case

A variation of the thermal power of the mHLS, spillage, heat recovery, and the nitrogen flow through the reactor was conducted in order to study respective impacts on the absorber temperature and the window temperature. As can be extracted from Fig. 8, the thermal power of the high flux solar simulator has a great influence on the temperatures in the system. A power reduction of 10% from 200 kW_{th} to 180 kW_{th} results in a drop of the absorber temperature of more than 50 K. On the other hand an improvement of the heat recovery fraction to 50% leads to a rise of the absorber temperature of more than 30 K.
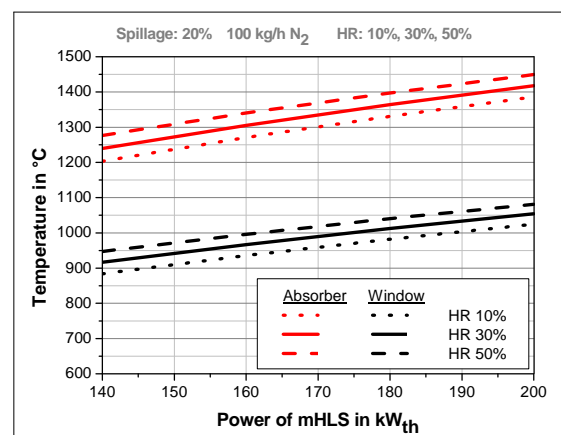

Fig. 8: Simulation results concerning the absorber temperature und the window temperature as a function of heat recovery and the thermal power of the mHLS

5

Absorber temperature and window temperature as a function of spillage are depicted in Fig. 9. Rising spillage results in decreased temperatures. Regarding the reference case a temperature drop of 65 K was calculated when spillage was set to 30%.
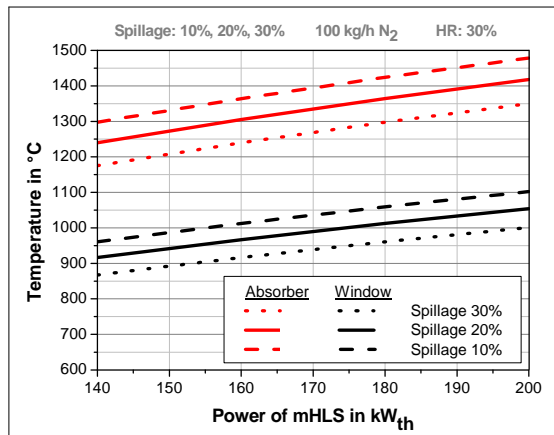

Fig. 9: Simulation results concerning the absorber temperature und the window temperature as a function of spillage and the thermal power of the mHLS

Similarly higher nitrogen flows lead to lower temperatures and vice versa. Based on the reference conditions a change of the nitrogen flow to 150 kg/h prohibits reaching the approached absorber temperatures higher than 1400 °C.
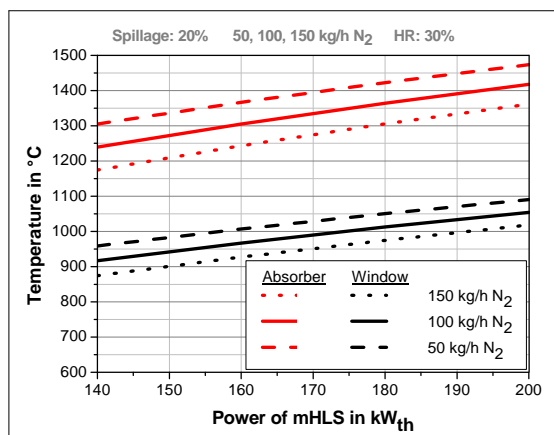

Fig. 10: Simulation results concerning the absorber temperature und the window temperature as a function of the nitrogen flow and the thermal power of the mHLS

The presented results of the simulation of a simplified reactor model under reference conditions suggest that reaching absorber temperatures of 1400 °C is possible with the considered configuration. Reducing spillage and increasing heat recovery promote higher absorber temperatures and provide important means of compensation of a potential decrease of the thermal power of the mHLS associated to potential lamp degradation effects. Moreover, a reduction of the nitrogen flow is favourable for high temperatures in the system. However, depending on applied figures additional cooling of the window may be necessary in order to avoid critical temperatures levels. Further refinement of the model should comprise the consideration of a real, not ideally black absorber, the substitution of the ideal isolation material, and a thorough assessment of temperature gradients in the window and the absorber, respectively.

6 Conclusion

This work shows the possibility of erecting a thermal stable water splitting ceria reactor for the achieved 1400 °C.

The reactor design itself is well-known and tested in several other experimental campaigns, which results in not expecting any special problems with the chosen design. Despite that, some changes have to be done, like changing the insulation material and the inlay for increasing the temperature stability of the reactor vessel. Additionally, it has been possible to increase the maximal reactive material to a volume of around 0.1 m³, while before that, the volume was around half of it.

Within the preliminary thermodynamic analysis the capability of the system to reach the needed 1400 °C within the reactor was shown. The analysis was preliminary, because the design had to be changed later on slightly. That means, the nitrogen flow could be controlling the absorber temperature as well as a decrease of spillage could increase the reactor's efficiency. Finally, the quartz glass window, which is the most sensitive part of the design, seems to stay below the maximal feasible temperature.

In the end, the reactor seems, based on this paper, able to fulfil all project's objectives.

As an outlook it

7 Acknowledgments

References

[1] C. Agrafiotis, M. Roeb, A. G. Konstandopoulos, L. Nalbandian a, V. T. Zaspalis, C. Sattler, P. Stobbe, and A. M. S. d, Solar water splitting for hydrogen production with monolithic reactors, 2005.

[2] F. Göhring, Modellierung und Simulation des Betriebsverhaltens eines Receiver-Reaktors zur solaren Wasserstoffproduktion, *Diploma Thesis*, Lehr- und Forschungsgebiet Solartechnik, RWTH Aachen, 2008.

[3] N. Knoblauch, L. Dörrer, P. Fielitz, M. Schmuecker, and G. Borchardt, Surface controlled reduction kinetics of

nominally undoped polycrystalline CeO2, *Physical Chemistry Chemical Physics*, vol. 17, pp. 5849-5860, 2015.

[4] M. Roeb, J. P. Säck, P. Rietbrock, C. Prahl, H. Schreiber, M. Neises, L. De Oliveira, D. Graf, M. Ebert, and W. Reinalter, Test operation of a 100kW pilot plant for solar hydrogen production from water on a solar tower, *Solar Energy*, vol. 85, pp. 634-644, 2011.

[5] J. P. Säck, M. Roeb, C. Sattler, R. Pitz-Paal, and A. Heinzel, Development of a system model for a hydrogen production process on a solar tower, *Solar Energy*, vol. 86, pp. 99-111, 2012.

[6]　　S. Abanades, P. Charvin, G. Flamant, and P. Neveu, Screening of water-splitting thermochemical cycles potentially attractive for hydrogen production by concentrated solar energy, *Energy*, vol. 31, pp. 2805-2822, 2006.

[7] W. C. Chueh, C. Falter, M. Abbott, D. Scipio, P. Furler, S. M. Haile, and A. Steinfeld, High-flux solar-driven thermochemical dissociation of CO2 and H2O using nonstoichiometric ceria, *Science*, vol. 330, pp. 1797-1801, 2010.

[8] J. R. Scheffe and A. Steinfeld, Thermodynamic Analysis of Cerium-Based Oxides for Solar Thermochemical Fuel Production, *Energy & Fuels*, vol. 26, pp. 1928-1936, 2012/03/15 2012.

[9] N. Itoh, M. A. Sanchez, W.-C. Xu, K. Haraya, and M. Hongo, Application of a membrane reactor system to thermal decomposition of CO2, *Application of Membrane Science*, vol. 77, pp. 245-253, 1993.

[10] F. Call, M. Roeb, M. Schmücker, H. Bru, D. Curulla-Ferre, C. Sattler, and R. Pitz-Paal, Thermogravimetric analysis of zirconia-doped ceria for thermochemical production of solar fuel, *American Journal of Analytical Chemistry*, vol. 4, pp. 37-45, 2013.

[11] VDI Heat Atlas, 2 ed. Berlin; Heidelberg: Springer-Verlag, 2010.